Radboud Repository

Radboud University Nijmegen

PDF hosted at the Radboud Repository of the Radboud University Nijmegen

The following full text is a publisher's version.

For additional information about this publication click this link.
http://hdl.handle.net/2066/208115

Please be advised that this information was generated on 2020-01-01 and may be subject to change.

Photoinduced Two-Body Loss of Ultracold Molecules

Arthur Christianen,[1] Martin W. Zwierlein,[2] Gerrit C. Groenenboom,[1] and Tijs Karman [3],*

[1]*Institute for Molecules and Materials, Radboud University, Heyendaalseweg 135, 6525 AJ Nijmegen, the Netherlands*
[2]*MIT-Harvard Center for Ultracold Atoms, Research Laboratory of Electronics, and Department of Physics,
Massachusetts Institute of Technology, Cambridge, Massachusetts 02139, USA*
[3]*ITAMP, Harvard-Smithsonian Center for Astrophysics, Cambridge, Massachusetts 02138, USA*

The lifetime of nonreactive ultracold bialkali gases was conjectured to be limited by sticky collisions amplifying three-body loss. We show that the sticking times were previously overestimated and do not support this hypothesis. We find that electronic excitation of NaK + NaK collision complexes by the trapping laser leads to the experimentally observed two-body loss. We calculate the excitation rate with a quasiclassical, statistical model employing *ab initio* potentials and transition dipole moments. Using longer laser wavelengths or repulsive box potentials may suppress the losses.

Ultracold dipolar gases have exciting applications across physics and chemistry [1,2]. They can be used for high-precision measurements that challenge the standard model of particle physics [3,4], to model or simulate quantum many-body physics [5–7], and to study and control chemical reactions [8,9]. There are also promising schemes for quantum computation using ultracold dipolar gases [10–12].

The first ultracold dipolar molecules in their absolute rovibronic and hyperfine ground state were realized by Ospelkaus *et al.* [13]. The KRb molecules used were reactive [9,14], which limits the lifetime of these ultracold gases. To avoid losses due to chemical reactions, several groups realized nonreactive ultracold dipolar gases of the bosonic $^{87}Rb^{133}Cs$ [15,16], $^{23}Na^{87}Rb$ [17], and the fermionic $^{23}Na^{40}K$ [18,19]. However, losses were still observed at about the same rate that would be expected of reactive molecules [20–22]. In all of these experiments, the lifetime of the gas in the crossed optical dipole trap was limited to a few seconds [18] or less [15–17]. Preventing this loss is of crucial importance for realizing higher molecular densities required for loading optical lattices and to improve the coherence time of ultracold molecules [23].

The loss mechanism in these nonreactive gases is not yet understood, but there are strong indications that the loss is caused by ultracold molecular collisions, which have been studied extensively in the literature [24]. Mayle *et al.* [25,26] proposed that the loss mechanism may be due to "sticky collisions," the formation of long-lived collision complexes. What actually happens to these complexes that causes loss of molecules from the trap is unknown and the subject of this Letter. We show that laser excitation of these complexes can explain the losses in the experiments.

Mayle *et al.* [25,26] propose a procedure to calculate the sticking time of a collision complex by calculating the density of states. Rice-Ramsperger-Kassel-Marcus

(RRKM) theory [27] relates the sticking time τ_{stick} of the collision to the density of states (DOS, ρ)

$$\tau_{stick} = 2\pi\hbar\rho. \tag{1}$$

Mayle *et al.* obtain the RRKM sticking time using multichannel quantum defect theory (MQDT) [[25,26], which treats the long range fully quantum mechanically but uses a simplified short range, parametrized by the DOS. However, in the accompanying paper [28] we show that there was an error in the DOS calculation, leading to sticking times of 2 to 3 orders of magnitude too large. A quasiclassical equation to accurately calculate the DOS for arbitrary potentials is found

$$\rho = \frac{g_{NJp}8\pi^{3+D/2}\hbar^3 C_{Nm}(2J+1)}{\Gamma(\frac{D}{2})}$$
$$\times \int G(\boldsymbol{q})[E - V(\boldsymbol{q})]^{(D/2)-1}d\boldsymbol{q}. \tag{2}$$

Here, E is the total energy in the system, J is the total angular momentum quantum number, p is the parity and $V(\boldsymbol{q})$ is the potential energy as a function of the Jacobi coordinates of the complex $\boldsymbol{q} = (R, r_1, r_2, \theta_1, \theta_2, \phi)$: the intermolecular distance R, the bond lengths r_1, r_2, the polar angles, θ_1, θ_2, and the dihedral angle, ϕ (see Ref. [29]). The complex has $D = 6$ internal degrees of freedom. The constant C_{Nm}, parity factor g_{NJp}, and geometry factor $G(\boldsymbol{q})$ are defined in the accompanying paper [28]. The factor $g_{NJp} = 1/2$ for collisions of heteronuclear diatoms.

We use Eq. (2) and the recently constructed, accurate potential energy surface (PES) [29] to calculate the DOS for the NaK + NaK system. These calculations result in a DOS of 0.37 μK^{-1} (for $J = 1$) and a sticking time of about

18 μs. We showed that this lifetime is not long enough for complex-diatom collisions to explain the experimental losses [28].

In this Letter, we show that the excitation of collision complexes by the trapping laser can explain the losses observed experimentally. In typical experiments, the diatoms are confined using a crossed optical dipole trap with lasers far red detuned (1064 nm [15,18,20,23] or 1550 nm [16,19,30]) from the molecular $X^1\Sigma^+ \to A^1\Sigma^+$ transition. However, the electronic excitation energies of the complex differ from those of the individual molecules and depend on the nuclear geometry of the complex. This means that, even though the laser is red detuned for the diatoms, the laser may electronically excite the collision complex.

Figure 1 shows the ground state and low-lying singlet excited states of NaK + NaK as a function of the intermolecular distance for a planar configuration of C_{2h} symmetry. Colors correspond to the different irreducible representations of the electronic states. The potentials were calculated *ab initio* using internally contracted multi-reference configuration interaction with MOLPRO [31], as described in more detail in the Supplemental Material [32]. The lowest two excited states correlate asymptotically to $X^1\Sigma^+ \to A^1\Sigma^+$ excitations of one of the NaK molecules. The third excited state of the complex correlates to both molecules excited to $a^3\Sigma^+$. Above that, we find excited states correlating to single $X^1\Sigma^+ \to B^1\Pi$ excitations, as well as simultaneous excitation of one molecule to $a^3\Sigma^+$ and the other to $b^3\Pi$. These highest two thresholds are nearly degenerate, and their order depends on the monomer bond
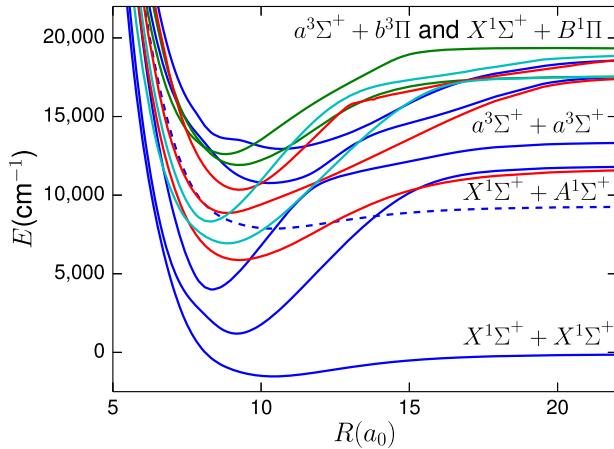

FIG. 1. A one-dimensional cut of the NaK + NaK PESs for the ground state and several excited states. The geometry is $r_1 = r_2 = 6.9 \, a_0$, $\theta_1 = 3\pi/4$, $\theta_2 = \pi/4$, $\phi = \pi$. *Ab initio* points were calculated over the entire range of R with intervals of $0.5 a_0$. The dashed line indicates the ground state energy curve plus the photon energy $\hbar\omega$ of a 1064 nm laser. With this geometry, the complex has a C_{2h} symmetry. The colors in the graph correspond to the irreducible representations of the states, blue for A_g, green for A_u, red for B_u, and cyan for B_g.

lengths. Higher excited states correlating to Na($S \to P$) transitions and more highly excited triplet states exist, but do not contribute to the absorption. We see that the excited-state potentials are more strongly bound than the ground-state potential; e.g., the first excited state potential has a well depth on the order of $12\,000$ cm^{-1} compared to the well depth of 4534 cm^{-1} of the ground-state potential [29]. The dashed line shows the ground-state potential shifted up by 1064 nm. This curve crosses four excited-state potentials in the region where the ground-state potential is attractive, indicating that these excited states can be reached. Furthermore, strong transition dipole moments (TDMs) to these excited states exist as the NaK $A^1\Sigma^+$ and $B^1\Pi$ excited states correlate to parallel and perpendicular dipole-allowed K($S \to P$) transitions.

This establishes that the energies of the excited states are low enough for trapping-laser-induced electronic transitions of collision complexes to occur. Next, we calculate the rates of these transitions to determine whether these transitions occur within the lifetime of a complex. This is not possible in the current MQDT framework, since this model does not explicitly treat the short range. Therefore, we develop a statistical model to calculate the laser excitation rates using *ab initio* short-range potentials.

The rate equation for laser excitation of the complex for a frozen geometry, q, from discrete state i to f is given by [37]

$$W_{i \to f}(q) = -\int d\omega \frac{b_{i \to f}(q, \omega) n}{c} \frac{dI}{d\omega}, \qquad (3)$$

where n is the particle density and $dI/d\omega$ is the spectral irradiance of the laser. The coefficient $b_{i \to f}$ is given by [37]

$$b_{i \to f}(q, \omega) = \frac{\pi}{3\epsilon_0 \hbar^2} \mu_{i \to f}^2(q) g(q, \omega), \qquad (4)$$

where $\mu_{i \to f}(q)$ is the TDM and $g(q, \omega)$ is the line shape of the transition. We set $n = n_c$, the number of collision complexes. We assume the collisions to be ergodic and use the same quasiclassical phase-space model used to calculate the sticking time. The nuclear motion is treated classically and electronic transitions can only occur when the ground-state electronic energy plus the photon energy matches the excited-state electronic energy, i.e., where the excited potentials cross the blue dashed line in Fig. 1.

We calculate the expectation value of $b_{i \to f}(q, \omega)$ over the accessible phase space as a function of ω. We assume the linewidth of the transition is small compared to the variation of the energy gap between the ground state and the excited state with geometry, $E_{\text{gap}}(q)$, and replace $g(q, \omega)$ by a delta function,

$$\langle b_{i \to f}(\boldsymbol{q}, \omega) \rangle_{\boldsymbol{q}} = \frac{g_{NJp} 8\pi^{3+D/2} \hbar^3 C_{Nm}(2J+1)}{3\epsilon_0 \hbar^2 \Gamma(\frac{D}{2})\rho}$$

$$\times \int d\boldsymbol{q} \, G(\boldsymbol{q}) [E_{\text{tot}} - V(\mathbf{y})]^{(D/2)-1} \mu_{i \to f}^2(\boldsymbol{q})$$

$$\times \delta\left(\frac{E_{\text{gap}}(\boldsymbol{q})}{\hbar} - \omega\right). \qquad (5)$$

The linewidth of the laser is also very small with respect to the variation of the excitation energy as a function of the geometry, such that $dI/d\omega$ can be replaced by $I_{\text{tot}} \delta(\omega_{\text{laser}} - \omega)$. Then, we sum over the electronic final states (f) to obtain

$$\frac{dn_c}{dt} = -n_c \sum_f \Gamma_{i \to f} = -n_c \sum_f \frac{I_{\text{tot}} \langle b_{i \to f}(\omega_{\text{laser}}) \rangle}{c}, \qquad (6)$$

where $\Gamma_{i \to f}$ is the excitation rate from state i to f. We define $\Gamma_{\text{laser}} = \sum_f \Gamma_{i \to f}$ and $\tau_{\text{laser}} = \Gamma_{\text{laser}}^{-1}$.

Before evaluating Eq. (6), we first qualitatively explore the properties of the TDM between the ground state and the low-lying excited states by again considering the one-dimensional cut for the C_{2h} configuration. Because of symmetry, only A_u and B_u states have nonzero TDMs with the ground state. We show the TDMs of the two lower-lying B_u states in Fig. 2. At long range, the $1B_u$ state corresponds to $(|AX\rangle - |XA\rangle)/\sqrt{2}$, the antisymmetric combination of $X^1\Sigma^+$ to $A^1\Sigma^+$ excitations in either molecule. The A excited state correlates to $K(S \to P)$ transitions. The molecular TDMs add constructively such that the $1B_u$ line strength approaches twice the line strength of the $S \to P$ transition of the K atom, $\mu^2 \sim 17 \ (ea_0)^2$. [38]. Asymptotically, the
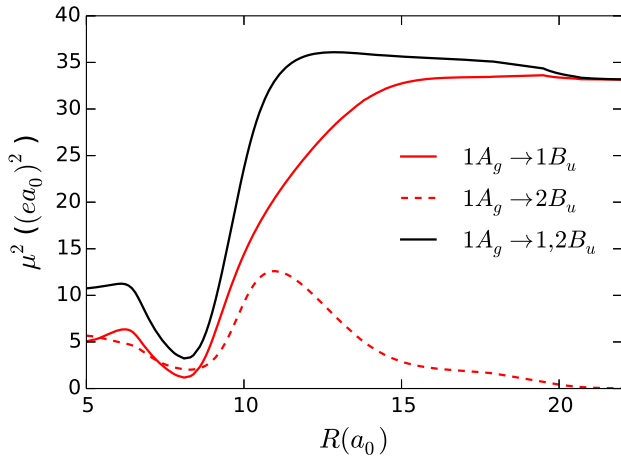

FIG. 2. A one-dimensional cut of two NaK + NaK squared-TDM surfaces. The geometry is $r_1 = r_2 = 6.9a_0$, $\theta_1 = 3\pi/4$, $\theta_2 = \pi/4$, and $\phi = \pi$. The TDMs plotted are those between the ground state and the first two excited states with B_u symmetry, corresponding to the red lines in Fig. 1. The black line corresponds to the sum of those two squared TDMs.

$2B_u$ state corresponds to $a^3\Sigma^+ + b^3\Pi$, which has zero TDM with the ground state. For $R < 20a_0$, these states mix such that the $1B_u$ TDM decreases and the $2B_u$ TDM increases, but the sum remains nearly constant. At yet shorter distances, $R < 10a_0$, short-range effects decrease all TDMs. The more highly excited states can be reached energetically only at very short range, where the TDMs drop substantially, such that the lowest three excited states dominate the excitation rate. In what follows, we include only these three excited states.

The evaluation of Eq. (5) requires global PESs and TDM surfaces, rather than the one-dimensional cuts discussed above. For the ground state, we use the GP9 PES from Ref. [29]. New PESs for the lowest three excited states are constructed to describe the gaps between the electronic energy levels. We also construct TDM surfaces for these excited states, and fit all surfaces using our machine-learning fitting method [29]. The details are described in the Supplemental Material [32].

For geometries with lower symmetry, the excited states exhibit many avoided crossings and conical intersections that complicate the electronic structure calculations. Conical intersections are expected to occur, e.g., from the many crossings observed in Fig. 2, and because the energetic ordering of electronic states switches between arrangements; the $a^3\Sigma^+ + a^3\Sigma^+$ state is the third excited state in the NaK + NaK arrangement, but the second excited state for $Na_2 + K_2$. Intersections occur at intermediate geometries. Near conical intersections, the TDM and potential energy vary rapidly with nuclear geometry, and the individual surfaces are difficult to fit accurately. However, we are interested in the laser-excitation rate, which is computed as a phase-space average summed over electronically excited states, and is less sensitive to the quality of the fits for individual electronic states.

The global TDM surfaces constructed here exhibit features similar to those observed at the C_{2h} symmetric configuration. At long range, the excited states have large TDMs due to their $K(S \to P)$ character. For lower-symmetry configurations, the lowest three excited states mix strongly, and the line strength distributes over the excited states, such that the individual squared TDMs vary with geometry, but the total remains approximately constant. At yet shorter range, the total TDM decreases.

Figure 3 shows the laser excitation rate as a function of the frequency at a trap depth of 10 μK. The colored lines indicate the laser transition rates to the individual excited states, the black line indicates the total. The grey shaded area indicates the error margin, which is estimated as described in the Supplemental Material [32]. The vertical dotted lines indicate wavelengths of 10 μm, 1550 nm, and 1064 nm. At 1064 nm, the loss rate is $\Gamma_{\text{laser}} = 3.3 \ \mu s^{-1}$, which corresponds to a lifetime for laser excitation of $\tau_{\text{laser}} = 0.30 \ \mu s$. At 1550 nm, the loss rate is reduced to 0.91 μs^{-1}, corresponding to a lifetime of 1.1 μs. At either
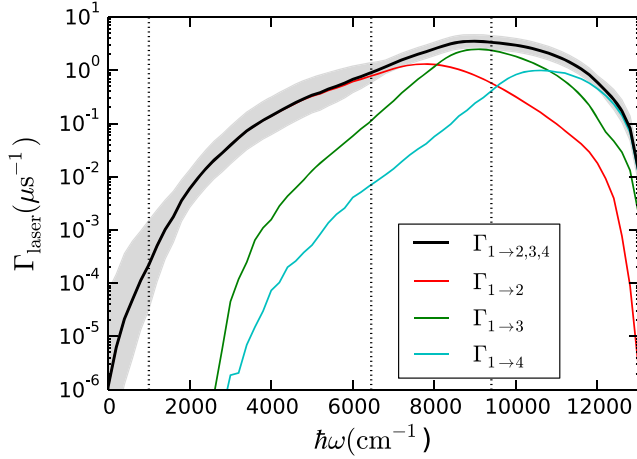
FIG. 3. The calculated laser excitation rate to the first three excited states as a function of the laser photon energy $\hbar\omega$. The vertical black dotted lines indicate the energies of the 10 μm, 1550 nm, and 1064 nm lasers. To calculate Γ_{laser}, a trap depth of 10 μK was used. For the above wavelengths, this corresponds to laser intensities of 12.6, 10.2, and 7.3 kW cm^{-2}, respectively. The grey shaded region indicates the error margin, which is estimated as described in the Supplemental Material [32].

FIG. 4. The laser-excitation lifetime, τ_{laser} (in the blue, left-hand axis, for a 1064 nm laser) and the half-life of NaK molecules in a crossed optical dipole trap, τ_{NaK} (in the red, right-hand axis), as a function of the laser intensity. The solid, dashed, and dashed-dotted red lines show results obtained using the full *ab initio* TDM surfaces for 1064 nm, 1550 nm, and 10 μm, respectively. The red shaded areas indicate the estimated error [32]. The vertical black dotted line indicates a typical experimental laser intensity of 10 kW cm^{-2}. We used an initial molecule density of 0.4×10^{11} cm^{-3}, temperature of 500 nK, and p-wave diatom-diatom collision rate of 3×10^{-11} cm^3 s^{-1}. The NaK lifetime, τ_{NaK}, accounts for both laser excitation and sticking-amplified three-body loss.

wavelength, the lifetime for laser excitation is much smaller than the sticking time, $\tau_{\text{laser}} \ll \tau_{\text{stick}} = 18$ μs. Hence, essentially all complexes formed undergo laser excitation before they dissociate, such that complex formation manifests as effective two-body loss, in agreement with experimental observations in Refs. [15,16,18,20,22]. Switching to a 10 μm laser wavelength would reduce the excitation rate by orders of magnitude to around 0.2 ms^{-1}, which is much slower than the complex dissociation rate.

Figure 4 shows the laser-excitation lifetime, τ_{laser}, of the complexes (in blue, left-hand axis) and the half-life of the NaK molecules in the trap τ_{NaK} (in red, right-hand axis), as a function of the laser intensity. The solid, dashed, and dashed-dotted lines show results for wavelengths of 1064 nm, 1550 nm, and 10 μm, respectively. The lifetime was calculated using an initial trap molecule density of 0.4×10^{11}cm^{-3}, temperature of 500 nK [18], and a diatom-diatom p-wave collision rate of 3×10^{-11} cm^3 s^{-1} based on multichannel quantum defect theory [26]. We include both the laser excitation loss mechanism and sticking-amplified three-body loss with a rate of 1.1×10^{-10} cm^{-3} s^{-1}, as described in Ref. [28]. The estimated lifetime of the complex with respect to complex-molecule collisions $\tau_{3b} = 1/[n(0)k_{3b}]$, where $n(0)$ is the initial molecular density and k_{3b} the molecule-complex collision rate. At 1064 nm and 1550 nm, in the typical range of experimental intensities, we find laser excitation leads to effective two-body loss, limited by the formation of collision complexes, and is insensitive to small changes in wavelength and intensity. For a 10 μm wavelength, however, the lifetime of
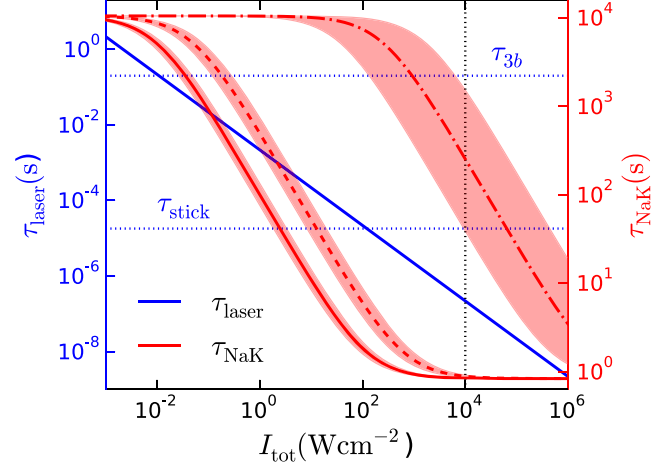
the molecules becomes orders of magnitude larger and strongly intensity-dependent. Changing the trapping laser wavelength to 10 μm emerges as a straightforward way to strongly reduce the losses. However, even at this wavelength, the laser excitation of collision complexes is dominant over sticking-amplified three-body loss.

Possibilities for reducing trapping-laser-induced loss of bialkali molecules are the following: (1) Box potentials: Rather than switching to very long wavelengths, a promising avenue may be to use shorter wavelengths to realize repulsive potential walls of blue-detuned trapping light [39], such that molecules are trapped between them in the dark. Such uniform box potentials have been realized for ultracold atoms, for both Bose-Einstein condensates [40] and Fermi gases [41]. (2) Preventing molecular collisions: If molecular collisions are suppressed, fewer collision complexes are formed that can be excited by the lasers. Several ways to prevent molecular collisions have been proposed, such as using optical lattices to confine the molecules [42], inducing repulsive interactions between colliding molecules using static [43], or using microwave fields [44,45]. (3) The trapping-laser excitation loss mechanism would be suppressed completely if the molecules were confined by nonoptical traps, such as a magnetic trap. This would require preparation of the molecules in a low-field seeking Zeeman state, and may require nonzero electron spin.

We note that any additional effects not taken into account here—such as an increased sticking time due to external fields or hyperfine coupling, or excitations to higher excited states—can only increase the loss. Such effects could increase trapping-laser-induced loss at lower intensities, while they do not affect the high-intensity limit where complex formation is the rate-limiting step, see Fig. 4.

To summarize, we find that experimentally observed losses of nonreactive ultracold molecules cannot be attributed to sticky collisions, but they can be explained by electronic excitation of collision complexes by the trapping laser. The loss can be reduced by using significantly lower intensities and longer wavelengths. The loss can be prevented by using a magnetic instead of an optical trap, repulsive box potentials, or by preventing molecular collisions. The theory is illustrated for NaK + NaK collisions. Other bialkalis, such as NaRb and RbCs, have comparable electronic structure and longer sticking times, such that we also expect trapping-laser-induced loss to be the major cause of losses for these systems.

[*]tijs.karman@cfa.harvard.edu

[1] L. D. Carr, D. DeMille, R. V. Krems, and J. Ye, New J. Phys. **11**, 055049 (2009).

[2] *Cold Molecules: Theory, Experiment, Applications*, edited by R. V. Krems, W. C. Stwalley, and B. Friedrich (CRC, Boca Raton, 2009).

[3] J. Baron, W. C. Campbell, D. DeMille, J. M. Doyle, G. Gabrielse, Y. V. Gurevich, P. W. Hess, N. R. Hutzler, E. Kirilov, I. Kozyryev, B. R. O'Leary, C. D. Panda, M. F. Parsons, E. S. Petrik, B. Spaun, A. C. Vutha, and A. D. West, Science **343**, 269 (2014).

[4] V. Andreev, D. G. Ang, D. DeMille, J. M. Doyle, G. Gabrielse, J. Haefner, N. R. Hutzler, Z. Lasner, C. Meisenhelder, B. R. O'Leary, C. D. Panda, A. D. West, E. P. West, and X. A. C. Wu, Nature (London) **562**, 355 (2018).

[5] A. Micheli, G. K. Brennen, and P. Zoller, Nat. Phys. **2**, 341 (2006).

[6] H. P. Büchler, E. Demler, M. Lukin, A. Micheli, N. Prokof'ev, G. Pupillo, and P. Zoller, Phys. Rev. Lett. **98**, 060404 (2007).

[7] N. R. Cooper and G. V. Shlyapnikov, Phys. Rev. Lett. **103**, 155302 (2009).

[8] R. V. Krems, Phys. Chem. Chem. Phys. **10**, 4079 (2008).

[9] S. Ospelkaus, K.-K. Ni, D. Wang, M. H. G. de Miranda, B. Neyenhuis, G. Quéméner, P. S. Julienne, J. L. Bohn, D. S. Jin, and J. Ye, Science **327**, 853 (2010).

[10] D. DeMille, Phys. Rev. Lett. **88**, 067901 (2002).

[11] S. F. Yelin, K. Kirby, and R. Côté, Phys. Rev. A **74**, 050301(R) (2006).

[12] K.-K. Ni, T. Rosenband, and D. D. Grimes, Chem. Sci. **9**, 6830 (2018).

[13] S. Ospelkaus, K.-K. Ni, G. Quéméner, B. Neyenhuis, D. Wang, M. H. G. de Miranda, J. L. Bohn, J. Ye, and D. S. Jin, Phys. Rev. Lett. **104**, 030402 (2010).

[14] K.-K. Ni, S. Ospelkaus, M. H. G. de Miranda, A. Pe'er, B. Neyenhuis, J. J. Zirbel, S. Kotochigova, P. S. Julienne, D. S. Jin, and J. Ye, Science **322**, 231 (2008).

[15] T. Takekoshi, L. Reichsöllner, A. Schindewolf, J. M. Hutson, C. R. Le Sueur, O. Dulieu, F. Ferlaino, R. Grimm, and H.-C. Nägerl, Phys. Rev. Lett. **113**, 205301 (2014).

[16] P. K. Molony, P. D. Gregory, Z. Ji, B. Lu, M. P. Köppinger, C. R. Le Sueur, C. L. Blackley, J. M. Hutson, and S. L. Cornish, Phys. Rev. Lett. **113**, 255301 (2014).

[17] M. Guo, B. Zhu, B. Lu, X. Ye, F. Wang, R. Vexiau, N. Bouloufa-Maafa, G. Quéméner, O. Dulieu, and D. Wang, Phys. Rev. Lett. **116**, 205303 (2016).

[18] J. W. Park, S. A. Will, and M. W. Zwierlein, Phys. Rev. Lett. **114**, 205302 (2015).

[19] F. Seeßelberg, N. Buchheim, Z.-K. Lu, T. Schneider, X.-Y. Luo, E. Tiemann, I. Bloch, and C. Gohle, Phys. Rev. A **97**, 013405 (2018).

[20] X. Ye, M. Guo, M. L. González-Martínez, G. Quéméner, and D. Wang, Sci. Adv. **4**, eaaq0083 (2018).

[21] M. Guo, X. Ye, J. He, M. L. González-Martínez, R. Vexiau, G. Quéméner, and D. Wang, Phys. Rev. X **8**, 041044 (2018).

[22] P. D. Gregory, M. D. Frye, J. A. Blackmore, E. M. Bridge, R. Sawant, J. M. Hutson, and S. L. Cornish, Nat. Commun. **10**, 3104 (2019).

[23] J. W. Park, Z. Z. Yan, H. Loh, S. A. Will, and M. W. Zwierlein, Science **357**, 372 (2017).

[24] G. Quéméner and P. S. Julienne, Chem. Rev. **112**, 4949 (2012).

[25] M. Mayle, B. P. Ruzic, and J. L. Bohn, Phys. Rev. A **85**, 062712 (2012).

[26] M. Mayle, G. Quéméner, B. P. Ruzic, and J. L. Bohn, Phys. Rev. A **87**, 012709 (2013).

[27] R. D. Levine, *Molecular Reaction Dynamics* (Cambridge University Press, Cambridge, England, 2005).

[28] A. Christianen, T. Karman, and G. C. Groenenboom, companion paper, Phys. Rev. A **100**, 032708 (2019).

[29] A. Christianen, T. Karman, R. A. Vargas-Hernández, G. C. Groenenboom, and R. V. Krems, J. Chem. Phys. **150**, 064106 (2019).

[30] F. Seeßelberg, X.-Y. Luo, M. Li, R. Bause, S. Kotochigova, I. Bloch, and C. Gohle, Phys. Rev. Lett. **121**, 253401 (2018).

[31] H.-J. Werner, P. J. Knowles *et al.*, Molpro: A package of *ab initio* programs, version 2015.1.

[32] See Supplemental Material at http://link.aps.org/supplemental/10.1103/PhysRevLett.123.123402 for details of the *ab initio* calculation, which includes Refs. [29,31,33–36].

[33] F. Weigend and R. Ahlrichs, Phys. Chem. Chem. Phys. **7**, 3297 (2005).

[34] M. Stein, Technometrics **29**, 143 (1987).

[35] F. O. Ellison, J. Am. Chem. Soc. **85**, 3540 (1963).

[36] C. Rasmussen and C. Williams, *Gaussian Processes for Machine Learning* (MIT Press, Cambridge, MA, 2006).

[37] R. C. Hilborn, Am. J. Phys. **50**, 982 (1982).

[38] D. K. Nandy, Y. Singh, B. P. Shah, and B. K. Sahoo, Phys. Rev. A **86**, 052517 (2012).

[39] N. Davidson, H. J. Lee, C. S. Adams, M. Kasevich, and S. Chu, Phys. Rev. Lett. **74**, 1311 (1995).

[40] A. L. Gaunt, T. F. Schmidutz, I. Gotlibovych, R. P. Smith, and Z. Hadzibabic, Phys. Rev. Lett. **110**, 200406 (2013).

[41] B. Mukherjee, Z. Yan, P. B. Patel, Z. Hadzibabic, T. Yefsah, J. Struck, and M. W. Zwierlein, Phys. Rev. Lett. **118**, 123401 (2017).

[42] M. H. G. de Miranda, A. Chotia, B. Neyenhuis, D. Wang, G. Quéméner, S. Ospelkaus, J. L. Bohn, J. Ye, and D. S. Jin, Nat. Phys. **7**, 502 (2011).

[43] M. L. González-Martínez, J. L. Bohn, and G. Quéméner, Phys. Rev. A **96**, 032718 (2017).

[44] T. Karman and J. M. Hutson, Phys. Rev. Lett. **121**, 163401 (2018).

[45] L. Lassablière and G. Quéméner, Phys. Rev. Lett. **121**, 163402 (2018).